

Robust Recovery of Subspace Structures by Low-Rank Representation

Guangcan Liu[‡], Zhouchen Lin[§], Senior Member, IEEE, Shuicheng Yan[‡],
Senior Member, IEEE, Ju Sun[†], Yong Yu[†], and Yi Ma[‡], Senior Member, IEEE

[‡] National University of Singapore, Singapore

[§] Microsoft Research Asia, Beijing, China

[†] Shanghai Jiao Tong University, Shanghai, China

[‡] University of Illinois at Urbana-Champaign, USA

Abstract—Data that arises from computer vision and image processing is often characterized by a mixture of multiple linear (or affine) subspaces, leading to the challenging problem of subspace segmentation. We observe that the heart of segmentation is to deal with the data that may not strictly follow subspace structures, i.e., to handle the data corrupted by noise. In this work we therefore address the subspace recovery problem. Given a set of data samples approximately drawn from a union of multiple subspaces, our goal is to segment the samples into their respective subspaces and correct the possible noise as well, i.e., our goal is to recover the subspace structures from corrupted data. To this end, we propose low-rank representation (LRR) for recovering a low-rank data matrix from corrupted observations. The recovery is performed by seeking the lowest-rank representation among all the candidates that can represent the data vectors as linear combinations of the basis in a given dictionary. LRR fits well the subspace recovery problem: When the data is noiseless, we prove that the lowest-rank representation exactly captures the true subspace structures; when the data may be corrupted by noise, the lowest-rank criterion can enforce noise correction such that LRR is robust. LRR solves a nuclear norm minimization problem, which is convex and can be solved efficiently. Under certain conditions, we further prove that the optimizer is unique and has a closed-form solution. Compared to previous subspace segmentation methods, most of which focus on segmentation only, LRR integrates data segmentation and noise correction into a unified framework, and thus achieves more accurate segmentation results in our experiments.

I. INTRODUCTION

In pattern analysis and signal processing, an underlying tenet is that the data contains some type of *structure* that enables intelligent representation and processing. So one usually needs a parametric model to characterize a given set of data. To this end, the well-known *linear subspaces*¹ are possibly the most common choice, mainly because they are easy to compute and are also often effective in real applications. Several types of visual data, such as motion [1], [2], [3], face [4] and texture [5], have been known to be well characterized by subspaces. Moreover, by applying the concept of reproducing kernel Hilbert space [6], one can easily extend the linear models to handle nonlinear data. So the

¹ There are two kinds of subspaces, linear and affine. We always use the term “subspace” to denote “linear subspace” in this work. In Section III-D.1, we will discuss how to deal with affine subspaces.

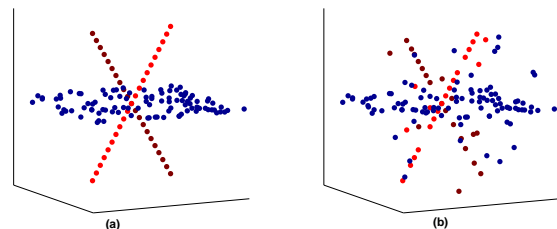


Fig. 1

A MIXTURE OF SUBSPACES CONSISTING OF A 2D PLANE AND TWO 1D LINES. (A) THE DATA VECTORS ARE EXACTLY SAMPLED FROM THE SUBSPACES. (B) THE DATA VECTORS ARE APPROXIMATELY SAMPLED FROM THE SUBSPACES.

subspace methods have been gaining much attention in recent years. For example, the widely used Principal Component Analysis (PCA) method and the recently established matrix completion [7], [8], [9], [10] methods are essentially based on the hypothesis that the data is approximately drawn from a low-rank subspace. However, a given data set can seldom be well described by a *single* subspace. A more reasonable model is to consider data as lying *near* several subspaces, namely, the data is considered as samples *approximately* drawn from a *mixture* of several low-rank subspaces, as shown in Fig.1.

The generality and importance of subspaces naturally lead to a challenging problem of *subspace segmentation*, whose goal is to segment (cluster or group) data into clusters with each cluster corresponding to a subspace. Subspace segmentation is an important data clustering problem as it arises in numerous research areas, including computer vision [3], [4], [11], [12], image processing [5], [13], [14], machine learning [15], [16] and system identification [17]. When the data is noiseless, i.e., the data samples are exactly sampled from the subspaces, several existing methods (e.g., [18], [19], [20]) are able to produce correct segmentation results under the assumption that the subspaces are independent. So, as pointed out by [3], [20], the main challenge of subspace segmentation is to

handle the *noise*² that possibly exists in data, i.e., to handle the data that may not strictly follow subspace structures. With this viewpoint, in this paper we therefore study the following *subspace recovery* problem with the purpose of achieving more accurate segmentation.

Problem 1.1 (Subspace Recovery): Given a set of data vectors *approximately* (i.e., the data may be corrupted by noise) drawn from a union of independent subspaces, correct the possible noise and segment all data vectors into their respective subspaces simultaneously.

A fundamental challenge in the above subspace recovery problem is the “chicken-and-egg” problem. If the data is already segmented properly, recovering the original data for each subspace would be performed perfectly by using the recently established Robust PCA (RPCA) method [7], [21]. Or, if the noise has been corrected, i.e., the data strictly follows subspace structures, segmenting the data into independent subspaces would be straightforward, as done in [18], [19], [20]. So the heart of subspace recovery is how to effectively handle the coupling between data segmentation and noise correction.

A. Previous Work

According to the mechanisms of representing the subspaces, existing works can be roughly divided into four main categories: mixture of Gaussian, factorization, algebraic and compressed sensing. Most existing methods solely target segmentation.

In statistical learning, mixed data is typically modeled as a set of independent samples drawn from a mixture of probabilistic distributions. As a single subspace can be well modeled by a (degenerated) Gaussian distribution, it is straightforward to assume that each probabilistic distribution is Gaussian, i.e., adopting a mixture of Gaussian model. Then the problem of segmenting the data is converted to a model estimation problem. The estimation can be performed either by using the Expectation Maximization (EM) algorithm to find a maximum likelihood estimate, as done in [22], or by iteratively finding a min-max estimate, as adopted by K-subspaces [11] and Random Sample Consensus (RANSAC) [13]. These methods are sensitive to noise. So several efforts have been made for improving their robustness, e.g., the Median K-flats [23] for K-subspaces, the work of [24] for RANSAC, and [5], [25] use a coding length to characterize a mixture of Gaussian. These refinements may introduce some robustness. Nevertheless, the problem is still not well solved due to the optimization difficulty, which is a bottleneck for these methods to achieve robustness.

Factorization based methods [18], [22] seek to approximate the given data matrix as a product of two matrices, such that the support pattern of one of the factors reveals the segmentation of the data vectors. In order to achieve robustness to noise, these methods modify the formulations by adding extra regularization terms. Nevertheless, such modifications

²In this paper, the noise usually refers to the *deviation* between model assumption and data. It could exhibit as white noise, outliers and missed entries in reality.

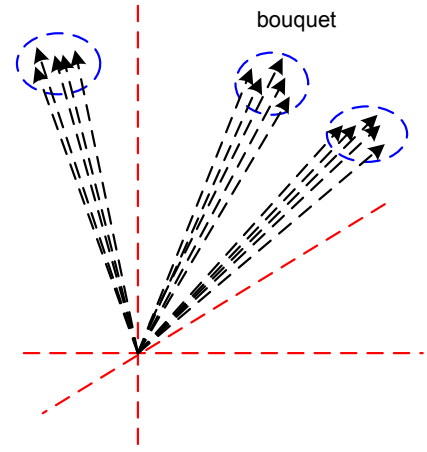


Fig. 2

ILLUSTRATING THE DATA STRUCTURE MODELED BY SR. THE DATA VECTORS ARE ASSUMED TO BE SAMPLED FROM A UNION OF “BOUQUETS” EACH OF WHICH CONTAINS A COLLECTION OF GAUSSIAN VECTORS WITH SMALL VARIANCE. EACH BOUQUET CORRESPONDS TO A CLUSTER.

usually lead to non-convex optimization problems, which need heuristic algorithms (often based on alternating minimization or EM-style algorithms) to solve. Getting stuck at local minima may depress their performances, especially when the data is grossly corrupted by noise. It will be shown that our method could be regarded as a robust generalization of the method in [18]. Our formulation is convex and can be solved efficiently.

Generalized Principal Component Analysis (GPCA) [26] presents an algebraic way to model the data drawn from a union of multiple subspaces. This method describes a subspace containing a data point by using the gradient of a polynomial at that point. Then subspace segmentation is made equivalent to fitting the data with polynomials. GPCA can guarantee the success of the segmentation under certain conditions, and it does not impose any restriction on the subspaces. However, this method is sensitive to noise due to the difficulty of estimating the polynomials from real data, which also causes the high computation cost of GPCA. Recently, Robust Algebraic Segmentation (RAS) [27] has been proposed to resolve the robustness issue of GPCA. However, the computation difficulty for fitting polynomials is unfathomably large. So RAS can make sense only when the data dimension is low and the number of subspaces is small.

The original goal of exploring *sparsity* is not for pattern recognition, but compression of signals, thus called *compressed sensing*. Due to the discriminative nature of the sparsest representation of a given data vector with respect to a dictionary, the work of [4] introduces the Sparse Representation (SR) method to face classification. Recently, [19] and [3] further introduce SR to subspace segmentation (unsupervised classification). SR based subspace segmentation methods use the sparsest representation produced by ℓ_1 -minimization to define the affinity matrix of an undirected graph. Then subspace segmentation is performed by spectral clustering algorithms such as Normalized Cuts (NCut) [28]. Under the assumption

that the data is noiseless and the subspaces are independent, [19] shows that the sparsest representation has the nature of high discrimination. Namely, the within-class affinities are sparse (but nonzero) and the between-class affinities are all zeros. This implies that the graph is well defined and easy to segment. The experimental reports in [19], [3] show that the SR based segmentation methods are quite competitive in reality. However, there are several questions on utilizing SR to model the *generic* subspace structures. First, according to the theoretical work of [14], the real mechanism of SR is not to model the generic subspace structures such as Fig.1, but a union of “bouquets” as shown in Fig.2. Although the bouquets could be roughly regarded as a special type of subspaces (a bouquet could be regarded as a concentrated subregion on a subspace), it is unclear whether or not SR could model well the generic subspace structures. Second, as SR finds the sparsest representation of each data vector individually, there is therefore no global constraint on its solution. So the method may be inaccurate at capturing the global structures of data (however, subspace is a type of global structure). This drawback can largely depress the performance when the data is grossly corrupted. Third, the pursuit of sparsity causes the sacrifice of high within-class homogeneity, which is also important for achieving accurate segmentation in an unsupervised environment. Because an affinity matrix with sparse within-class homogeneity may not produce accurate segmentation, especially when the data is grossly corrupted, it should be more helpful for clustering if the within-class affinities are dense and the between-class affinities are zero (similar to the “block-sparse” property discussed in [29]).

B. Our Contributions

In this work, we propose a novel method, called *low-rank representation* (LRR) [20], to recover the subspace structures from corrupted data. Given a set of data vectors each of which can be represented as a linear combination of the basis in a dictionary, LRR aims at finding the *lowest-rank* representation of all data *jointly*. By choosing an appropriate dictionary, the lowest-rank representation has the nature of both high within-class homogeneity and large between-class margin: When the data is noiseless, we prove that the lowest-rank representation corresponds to an affinity matrix which has *dense* within-class affinities and *zero* between-class affinities. That is, the lowest-rank representation exactly reveals the segmentation of data. We prove that such a lowest-rank representation can be found by solving a nuclear norm minimization problem, which has a unique and closed-form minimizer. For corrupted data, since the noise will largely increase the rank as shown in matrix competition problems (e.g., [7], [8], [9]), the lowest-rank criterion can enforce noise correction such that LRR could produce robust recovery to the subspace structures. In summary, the contributions of this work include:

- We introduce the problem of subspace recovery that integrates segmentation and noise correction into a unified framework. Based on the studies of this problem, we develop a simple yet effective subspace segmentation algorithm that outperforms the state-of-the-art algorithms in handling corrupted data.

- Our work extends the recovery of corrupted data from a single subspace [9] to multiple subspaces. Compared to [29], which requires the basis of subspaces to be known for handling the corrupted data from multiple subspaces, our method is *autonomous*, i.e., no extra clean data is required.
- When the data is noiseless, we prove that the lowest-rank representation can be found by solving a nuclear norm minimization problem. With some mild assumptions, we further prove that the minimization problem has a unique and closed-form minimizer. These results are also useful for other nuclear norm related problems.

C. Paper Organization

The remainder of this paper is organized as follows. Section II summarizes the usage of mathematical notations and the formulation of the problem we study. Section III introduces the theorems and algorithms of LRR. Section IV studies the problem of subspace recovery. Section V presents the experimental results and Section VI concludes this paper.

II. SUMMARY OF NOTATIONS AND PROBLEM STATEMENT

A. Summary of Notations

In this work, matrices and vectors are represented with capital and lowercase symbols, respectively. The scalars are denoted by Greek letters. In particular, \mathbf{I} is used to denote the identity matrix, seven lowercases d, i, j, m, n, k and l are kept to denote natural numbers, and the entries (of matrices and vectors) are denoted by using $[\cdot]_{ij}$ with subscripts. For instance, V is a matrix and $[V]_{ij}$ its (i, j) -th entry. Likewise v is a vector and $[v]_i$ its i -th component. For any matrix V , $[V]_{i,:}$ and $[V]_{:,j}$ denote its i -th row and j -th column, respectively. A collection of matrices (vectors) are represented as capital (lowercase) with subscripts. For example, V_1, V_2, \dots, V_k (or v_1, v_2, \dots, v_k) are a collection of matrices (or vectors). Sometimes, for ease of presentation, the concatenation of a collection of matrices along column (or row) is denoted by $[V_1, V_2, \dots, V_k]$ (or $[V_1; V_2; \dots; V_k]$). The block-diagonal matrix formed by a collection of matrices V_1, V_2, \dots, V_k is denoted by:

$$\text{diag}(V_1, V_2, \dots, V_k) = \begin{bmatrix} V_1 & 0 & 0 & 0 \\ 0 & V_2 & 0 & 0 \\ 0 & 0 & \ddots & 0 \\ 0 & 0 & 0 & V_k \end{bmatrix}.$$

A variety of norms on matrices and vectors will be used. $\|v\|_0$, $\|v\|_1$ and $\|v\|_2$ are ℓ_0 -norm, ℓ_1 -norm and ℓ_2 -norm of a vector v , respectively. The matrix ℓ_0 -norm and ℓ_1 -norm are denoted by $\|V\|_0$ (number of nonzero entries) and $\|V\|_1 = \sum_{i,j} |[V]_{ij}|$, respectively. The matrix ℓ_∞ -norm is defined as $\|V\|_\infty = \max_{i,j} |[V]_{ij}|$. The spectral norm of a matrix V is denoted by $\|V\|$, i.e., $\|V\|$ is the maximum singular value of V . The Hadamard product between two matrices is $V \circ N$, where $[V \circ N]_{ij} = [V]_{ij}[N]_{ij}$. The Euclidean inner product between two matrices is $\langle V, N \rangle = \text{tr}(V^T N)$, where V^T is the transpose of a matrix and $\text{tr}(\cdot)$ is the trace of a square

matrix. For a non-square matrix M , assuming $M = [M_1, M_2]$ or $M = [M_1; M_2]$, where M_1 is square, we define $\text{tr}(M) = \text{tr}(M_1)$. The Frobenious norm and the *nuclear norm* [30] (the sum of singular values of a matrix) are denoted by $\|V\|_F$ and $\|V\|_*$, respectively.

The ℓ_2/ℓ_1 -norm of a matrix is defined by:

$$\|V\|_{2,1} = \sum_j \sqrt{\sum_i [V]_{ij}^2}. \quad (1)$$

Finally, we use calligraphic letters to denote subspaces, e.g., we use $\{\mathcal{S}_1, \mathcal{S}_2, \dots, \mathcal{S}_k\}$ to denote a collection of k subspaces. The sum and direct sum of a collection of k independent subspaces are denoted by $\sum_{i=1}^k \mathcal{S}_i$ and $\oplus_{i=1}^k \mathcal{S}_i$, respectively. We also adopt the conventions of using $\text{span}(A)$ to denote the linear space spanned by the columns of a matrix A , using $x \in \text{span}(A)$ to denote that the vector x belongs to the space $\text{span}(A)$, and using $X \in \text{span}(A)$ to denote that all column vectors of X belong to $\text{span}(A)$.

B. Problem Statement

Problem 1.1 only roughly describes what we want to study. More precisely, this paper addresses the following problem. Let X^0 be a set of sufficiently dense samples *exactly* drawn from a union of k subspaces $\{\mathcal{S}_i\}_{i=1}^k$ of unknown dimensions. Without loss of generality, we assume that $X^0 = [X_1^0, X_2^0, \dots, X_k^0]$ and X_i^0 is collection of n_i samples from the i -th subspace \mathcal{S}_i . Since the sampling is dense enough, each X_i^0 is self-expressive: $X_i^0 = X_i^0 Z_i^0$, where Z_i^0 is an $n_i \times n_i$ coefficient matrix. By constructing a block-diagonal matrix $Z^0 = \text{diag}(Z_1^0, Z_2^0, \dots, Z_k^0)$, the above data generation process can be summarized by

$$X^0 = X^0 Z^0.$$

Then the goal of subspace recovery is to recover the block-diagonal coefficient matrix Z^0 and the original low-rank data matrix X^0 from corrupted observations, i.e.,

Problem 2.1 (Subspace Recovery): Given a set of observation vectors X contaminated by noise E^0 , i.e.,

$$X = X^0 + E^0,$$

our goal is to recover Z^0 (segmentation) and X^0 (noise correction) simultaneously.

We consider the problem under three assumptions of increasing practicality and difficulty.

Assumption 1. The subspaces are of low-rank and *independent*³, and the data is noiseless (i.e., $E^0 = 0$).

Assumption 2. The subspaces are of low-rank and independent, a fraction of the data vectors are grossly corrupted by large noise and the others are noiseless.

Assumption 3. The subspaces are of low-rank and independent, a fraction of the data vectors are grossly corrupted and the others are contaminated by small noise.

³The subspaces are independent if and only if $\mathcal{S}_i \cap \sum_{j \neq i} \mathcal{S}_j = \{0\}$ (or $\sum_{i=1}^k \mathcal{S}_i = \oplus_{i=1}^k \mathcal{S}_i$). When the subspaces are low-rank and the data vectors are high-dimensional, the independent assumption is roughly equal to the disjoint assumption; that is $\mathcal{S}_i \cap \mathcal{S}_j = \{0\}, \forall i \neq j$.



Fig. 3

AN ILLUSTRATION OF OUR THREE ASSUMPTIONS. HERE WE PLOT THE MAGNITUDE OF NOISE AS A FUNCTION OF THE INDEX OF DATA VECTOR.

The independence assumption is mild, because it is usually true, especially when the subspaces are of low-rank. It is also necessary, because the data generation process will be “ambiguous” if the subspaces have nonzero (nonempty) intersections. So what is critical is that the real data may not strictly follow subspace structures, i.e., there may exist errors (noise) in data. Actually, the above three assumptions correspond to three kinds of distributions of the noise E^0 , as shown in Fig.3.

III. LOW-RANK REPRESENTATION FOR RECOVERING LOW-RANK MATRICES

For ease of understanding, in this section we abstractly present the LRR method for recovering the low-rank matrix X^0 from a corrupted observation matrix $X = X^0 + E^0$ (each column of X is an observation vector). The detailed methods for handling the subspace recovery problem are deferred until Section IV.

A. Low-Rank Representation

In order to recover the low-rank matrix X^0 from the given observation matrix X corrupted by noise, it is straightforward to consider the following regularized rank minimization problem:

$$\begin{aligned} \min_{D, E} \quad & \text{rank}(D) + \lambda \|E\|_\ell, \\ \text{s.t.} \quad & X = D + E, \end{aligned} \quad (2)$$

where $\lambda > 0$ is a parameter and $\|\cdot\|_\ell$ is some kind of regularization strategy, such as the ℓ_1 -norm adopted by [9], [21], for characterizing the noise E^0 . The minimizer D^* (with respect to the variable D) gives a low-rank recovery of the original data X^0 . The above formulation is adopted by the recently established Robust PCA (RPCA) method [9], [21] which has been used to achieve the state-of-the-art performance in several applications (e.g., [31]). However, this formulation implicitly

assumes that the underlying data structure is a single low-rank subspace. When the data is drawn from a union of multiple subspaces, denoted as $\mathcal{S}_1, \mathcal{S}_2, \dots, \mathcal{S}_k$, the PRCA method actually treats the data as being sampled from a single subspace defined by

$$\mathcal{S} = \sum_{i=1}^k \mathcal{S}_i.$$

The specifics of the individual subspaces are not well considered, so the recovery may be inaccurate.

To better handle the mixed data, here we suggest a more general rank minimization problem defined as follows:

$$\begin{aligned} \min_{Z, E} \quad & \text{rank}(Z) + \lambda \|E\|_\ell, \\ \text{s.t.} \quad & X = AZ + E, \end{aligned} \quad (3)$$

where A is a ‘‘dictionary’’ that linearly spans the data space. We call the minimizer Z^* (with regard to the variable Z) the ‘‘lowest-rank representation’’ of data X with respect to a dictionary A . After obtaining an optimal solution (Z^*, E^*) , we could recover the original data by using AZ^* (or $X - E^*$). Since $\text{rank}(AZ^*) \leq \text{rank}(Z^*)$, AZ^* is also a low-rank recovery to the original data X^0 . By setting $A = \mathbf{I}$, the formulation (3) falls back to (2). So our LRR method could be regarded as a generalization of RPCA that essentially uses the standard basis as the dictionary. By choosing an appropriate dictionary A , as we will see, the lowest-rank representation also reveals the segmentation of data such that LRR could handle well the data drawn from a mixture of multiple subspaces.

B. Analysis on the LRR Problem

The optimization problem (3) is difficult to solve due to the discrete nature of the rank function. For ease of exploration, we begin with the ‘‘ideal’’ case that the data is noiseless. That is, we consider the following optimization problem:

$$\begin{aligned} \min_Z \quad & \text{rank}(Z), \\ \text{s.t.} \quad & X = AZ. \end{aligned} \quad (4)$$

It is easy to see that the solution to (4) is not unique. As a common practice in rank minimization problems, we replace the rank function with the nuclear norm, resulting in the following convex optimization problem:

$$\begin{aligned} \min_Z \quad & \|Z\|_*, \\ \text{s.t.} \quad & X = AZ. \end{aligned} \quad (5)$$

We will show that the solution to (5) is also a solution to (4) and this special solution is useful for subspace segmentation.

In the following, we shall show some general properties of the minimizer to problem (5). The following general conclusions form the foundations of our LRR method.

1) *Uniqueness of the Minimizer:* The nuclear norm is convex, but not strongly convex. So it is possible that problem (5) has multiple optimal solutions. Fortunately, it can be proven that the minimizer to problem (5) is *always* uniquely defined by a closed form. This is summarized in the following theorem.

Theorem 3.1 (Uniqueness): Assume $A \neq 0$ and $X = AZ$ have feasible solutions, i.e., $X \in \text{span}(A)$. Then

$$Z^* = V_A(V_A^T V_A)^{-1} V_X^T, \quad (6)$$

is the unique minimizer to problem (5), where V_X and V_A are calculated as follows: Compute the skinny Singular Value Decomposition (SVD)⁴ of $[X, A]$, denoted as $[X, A] = U\Sigma V^T$, and partition V as $V = [V_X; V_A]$ such that $X = U\Sigma V_X^T$ and $A = U\Sigma V_A^T$.

From the above theorem we have the following three corollaries. First, it shows that problem (5) is a good surrogate of problem (4).

Corollary 3.1: Assume $A \neq 0$ and $X = AZ$ have feasible solutions. Let Z^* be the minimizer to problem (5), then $\text{rank}(Z^*) = \text{rank}(X)$ and Z^* is also a globally optimal solution to problem (4).

Proof: By (6), we have $\text{rank}(Z^*) = \text{rank}(V_X)$. By the definition of V_X , we have $\text{rank}(X) = \text{rank}(U\Sigma V_X^T) = \text{rank}(V_X)$. Hence, $\text{rank}(Z^*) = \text{rank}(X)$. At the same time, for any feasible solution Z to problem (4), we have $\text{rank}(Z) \geq \text{rank}(AZ) = \text{rank}(X)$. So, Z^* is also optimal to problem (4). ■

Second, when the matrix A is of full row rank, the closed-form solution defined by (6) can be represented in a simpler form.

Corollary 3.2: Suppose the matrix A has full row rank, then

$$Z^* = A^T(AA^T)^{-1}X,$$

is the unique minimizer to problem (5), where $A^T(AA^T)^{-1}$ is the *generalized inverse* of A .

Third, when the data matrix itself is used as the dictionary, i.e., $A = X$, the solution to problem (5) falls back to the outputs of a factorization based method. This is stated in the following corollary and has been proven by Wei and Lin [32].

⁴For an $m \times n$ matrix M (without loss of generality, assuming $m \leq n$), its SVD is defined by

$$M = U[\Sigma, 0]V^T,$$

where U (with dimension $m \times m$) and V (with dimension $n \times n$) are orthogonal matrices and $\Sigma = \text{diag}(\sigma_1, \sigma_2, \dots, \sigma_m)$ with $\{\sigma_i\}_{i=1}^m$ being singular values. The SVD defined in this way is also called the *full* SVD. If we only keep the positive singular values and their corresponding singular vectors, the reduced form is called the *skinny* SVD. For a matrix M of rank r , its skinny SVD is computed by

$$M = U_r \Sigma_r V_r^T,$$

where $U_r^T U_r = V_r^T V_r = \mathbf{I}_r$, $\Sigma_r = \text{diag}(\sigma_1, \sigma_2, \dots, \sigma_r)$ and $\sigma_i > 0, 1 \leq i \leq r$. The SVD of a matrix is not unique if some singular values are identical. However, the non-uniqueness of the SVD does not affect the uniqueness of the closed-form solution (6).

Corollary 3.3: Assume $X \neq 0$. Then the following optimization problem

$$\begin{aligned} \min_Z \quad & \|Z\|_*, \\ \text{s.t.} \quad & X = XZ, \end{aligned}$$

has a unique minimizer

$$Z^* = \text{SIM}(X), \quad (7)$$

where $\text{SIM}(X) = V_X V_X^T$ is called the Shape Interaction Matrix (SIM) [18] in computer vision and $X = U_X \Sigma_X V_X^T$ is the skinny SVD of X .

The proof of Theorem 3.1 is based on the following three lemmas.

Lemma 3.1: Let U , V and M be matrices of compatible dimensions. Suppose both U and V have orthogonal columns, i.e., $U^T U = \mathbf{I}$ and $V^T V = \mathbf{I}$ ⁵, then we have

$$\|M\|_* = \|UMV^T\|_*.$$

Proof: Let the full SVD of M be $M = U_M \Sigma_M V_M^T$, then $UMV^T = (UU_M) \Sigma_M (VV_M)^T$. As $(UU_M)^T (UU_M) = \mathbf{I}$ and $(VV_M)^T (VV_M) = \mathbf{I}$, $(UU_M) \Sigma_M (VV_M)^T$ is actually the SVD of UMV^T . By the definition of the nuclear norm, we have $\|M\|_* = \text{tr}(\Sigma_M) = \|UMV^T\|_*$. ■

Lemma 3.2: For any four matrices B , C , D and F of compatible dimensions, we have

$$\left\| \begin{bmatrix} B & C \\ D & F \end{bmatrix} \right\|_* \geq \|B\|_*,$$

where the equality holds if and only if $C = 0, D = 0$ and $F = 0$.

Proof: Lemma 10 of [33] directly leads to the above conclusion. ■

Lemma 3.3: Let U , V and M be given matrices of compatible dimensions. Suppose both U and V have orthogonal columns, i.e., $U^T U = \mathbf{I}$ and $V^T V = \mathbf{I}$, then the following optimization problem

$$\begin{aligned} \min_Z \quad & \|Z\|_*, \\ \text{s.t.} \quad & U^T ZV = M, \end{aligned} \quad (8)$$

has a unique minimizer

$$Z^* = UMV^T.$$

Proof: First, we prove that $\|M\|_*$ is the minimum objective function value and $Z^* = UMV^T$ is a minimizer. For any feasible solution Z , let $Z = U_Z \Sigma_Z V_Z^T$ be its full SVD. Let $B = U^T U_Z$ and $C = V_Z^T V$. Then the constraint $U^T ZV = M$ is equal to

$$B \Sigma_Z C = M. \quad (9)$$

Since $BB^T = \mathbf{I}$ and $C^T C = \mathbf{I}$, we can find the orthogonal complements⁶ B_\perp and C_\perp such that

$$\begin{bmatrix} B \\ B_\perp \end{bmatrix} \quad \text{and} \quad [C, C_\perp]$$

⁵Note here that U and V may not be orthogonal, namely, $UU^T \neq \mathbf{I}$ and $VV^T \neq \mathbf{I}$.

⁶When B and/or C are already orthogonal matrices, i.e., $B_\perp = \emptyset$ and/or $C_\perp = \emptyset$, our proof is still valid.

are orthogonal matrices. According to the unitary invariance of the nuclear norm, Lemma 3.2 and (9), we have

$$\begin{aligned} \|Z\|_* &= \|\Sigma_Z\|_* = \left\| \begin{bmatrix} B \\ B_\perp \end{bmatrix} \Sigma_Z [C, C_\perp] \right\|_* \\ &= \left\| \begin{bmatrix} B \Sigma_Z C & B \Sigma_Z C_\perp \\ B_\perp \Sigma_Z C & B_\perp \Sigma_Z C_\perp \end{bmatrix} \right\|_* \\ &\geq \|B \Sigma_Z C\|_* = \|M\|_*, \end{aligned}$$

Hence, $\|M\|_*$ is the minimum objective function value of problem (8). At the same time, Lemma 3.1 proves that $\|Z^*\|_* = \|UMV^T\|_* = \|M\|_*$. So $Z^* = UMV^T$ is a minimizer to problem (8).

Second, we prove that $Z^* = UMV^T$ is the unique minimizer. Assume that $Z_1 = UMV^T + H$ is another optimal solution. By $U^T Z_1 V = M$, we have

$$U^T H V = 0. \quad (10)$$

Since $U^T U = \mathbf{I}$ and $V^T V = \mathbf{I}$, similar to above, we can construct two orthogonal matrices: $[U, U_\perp]$ and $[V, V_\perp]$. By the optimality of Z_1 , we have

$$\begin{aligned} \|M\|_* &= \|Z_1\|_* = \|UMV^T + H\|_* \\ &= \left\| \begin{bmatrix} U^T \\ U_\perp^T \end{bmatrix} (UMV^T + H) [V, V_\perp] \right\|_* \\ &= \left\| \begin{bmatrix} M & U^T H V_\perp \\ U_\perp^T H V & U_\perp^T H V_\perp \end{bmatrix} \right\|_* \\ &\geq \|M\|_*. \end{aligned}$$

According to Lemma 3.2, the above equality can hold if and only if

$$U^T H V_\perp = U_\perp^T H V = U_\perp^T H V_\perp = 0.$$

Together with (10), we conclude that $H = 0$. So the optimal solution is unique. ■

The above lemma allows us to get closed-form solutions to a class of nuclear norm minimization problems. This leads to a simple proof of Theorem 3.1.

Proof: (of Theorem 3.1) Since $X \in \text{span}(A)$, we have $\text{rank}([X, A]) = \text{rank}(A)$. By the definitions of V_X and V_A (see Theorem 3.1), it can be concluded that the matrix V_A^T has full row rank. That is, if the skinny SVD of V_A^T is $U_1 \Sigma_1 V_1^T$, then U_1 is an orthogonal matrix. Through some simple computations, we have

$$V_A (V_A^T V_A)^{-1} = V_1 \Sigma_1^{-1} U_1^T. \quad (11)$$

Also, it can be calculated that the constraint $X = AZ$ is equal to $V_X^T = V_A^T Z$, which is also equal to $\Sigma_1^{-1} U_1^T V_X^T = V_1^T Z$. So problem (5) is equal to the following optimization problem:

$$\begin{aligned} \min_Z \quad & \|Z\|_*, \\ \text{s.t.} \quad & V_1^T Z = \Sigma_1^{-1} U_1^T V_X^T. \end{aligned}$$

By Lemma 3.3 and (11), problem (5) has a unique minimizer

$$\begin{aligned} Z^* &= V_1 \Sigma_1^{-1} U_1^T V_X^T \\ &= V_A (V_A^T V_A)^{-1} V_X^T. \end{aligned}$$

■

2) *Discrimination and Homogeneity of the Minimizer*: As mentioned in Section III-A, the lowest-rank representation can reveal the true segmentation results by choosing an appropriate dictionary. Namely, when the columns of A and X are exactly sampled from independent subspaces, the minimizer to problem (5) has the nature of large between-class margin and high within-class homogeneity. Let $\{\mathcal{S}_1, \mathcal{S}_2, \dots, \mathcal{S}_k\}$ be a collection of k subspaces, each of which has a rank (dimension) of $r_i > 0$. Also, let $A = [A_1, A_2, \dots, A_k]$ and $X = [X_1, X_2, \dots, X_k]$. Then we have the following theorem.

Theorem 3.2: Assume that A_i is collection of m_i basis of the i -th subspace \mathcal{S}_i and X_i is collection of n_i samples from \mathcal{S}_i and the sampling of each A_i is sufficient such that $\text{rank}(A_i) = r_i$. If the subspaces are independent then the minimizer to problem (5) is block-diagonal:

$$Z^* = \begin{bmatrix} Z_1^* & 0 & 0 & 0 \\ 0 & Z_2^* & 0 & 0 \\ 0 & 0 & \ddots & 0 \\ 0 & 0 & 0 & Z_k^* \end{bmatrix},$$

where Z_i is an $m_i \times n_i$ coefficient matrix with $\text{rank}(Z_i^*) = \text{rank}(X_i)$, $\forall i$.

This theorem and Corollary 3.3 straightforwardly lead to the following corollary, part of which has been proven in [18].

Corollary 3.4: Assume that the sampling of each X_i is sufficient such that $\text{rank}(X_i) = r_i$. If the subspaces are independent then the shape interaction matrix $\text{SIM}(X)$ is a block-diagonal matrix that has exactly k blocks, the i -th block is of size $n_i \times n_i$, and the rank of the i -th block is r_i .

The above two conclusions show that the lowest-rank representation can reveal the true subspace membership by choosing a dictionary (e.g., $A = X$) that contains the basis of the subspaces. It is also worth noting that the claim of $\text{rank}(Z_i^*) = \text{rank}(X_i)$ guarantees the high within-class homogeneity of Z_i^* . This is different from SR, which is prone to obtain a ‘‘trivial’’ solution if $A = X$, because the sparsest representation is an identity matrix in this case. The proof of Theorem 3.2 is based on the following lemma.

Lemma 3.4 ([34], Lemma 3.2): For any four matrices B , C , D and F of compatible dimensions, we have

$$\left\| \begin{bmatrix} B & C \\ D & F \end{bmatrix} \right\|_* \geq \left\| \begin{bmatrix} B & 0 \\ 0 & F \end{bmatrix} \right\|_* = \|B\|_* + \|F\|_*.$$

The above lemma allows us to lower-bound the objective value at any solution Z by the value of the block-diagonal restriction of Z . This leads to a simple proof of Theorem 3.2:

Proof: (of Theorem 3.2) Let Z^* be the optimizer to problem (5). Form a block-diagonal matrix W by setting

$$[W]_{ij} = \begin{cases} [Z]_{ij}, & [A]_{:,i} \text{ and } [X]_{:,j} \text{ belong to} \\ & \text{the same subspace,} \\ 0, & \text{otherwise.} \end{cases}$$

Write $Q = Z^* - W$. For any data vector $[X]_{:,j}$, without loss of generality, suppose $[X]_{:,j}$ belongs to the i -th subspace; i.e., $[AZ^*]_{:,j} \in \mathcal{S}_i$. Then by construction, we have $[AW]_{:,j} \in \mathcal{S}_i$ and $[AQ]_{:,j} \in \oplus_{m \neq i} \mathcal{S}_m$. But $[AQ]_{:,j} = [X]_{:,j} - [AW]_{:,j} \in$

\mathcal{S}_i . By independence, we have $\mathcal{S}_i \cap \oplus_{m \neq i} \mathcal{S}_m = \{0\}$, and so $[AQ]_{:,j} = 0$, $\forall j$.

Hence, $AQ = 0$, and W is feasible for (5). By Lemma 3.4, we have $\|Z^*\|_* \geq \|W\|_*$. Also, by the uniqueness of the minimizer (see Theorem 3.1), we conclude that $Z^* = W$ and hence Z^* is block-diagonal.

Again, by the uniqueness of the minimizer Z^* , we can conclude that for all i 's, Z_i^* is also the unique minimizer to the following optimization problem:

$$\begin{aligned} \min_J \quad & \|J\|_*, \\ \text{s.t.} \quad & X_i = A_i J. \end{aligned}$$

By Corollary 3.1, we conclude that $\text{rank}(Z_i^*) = \text{rank}(X_i)$. ■

3) *Sensitivity to Perturbations*: In real applications, our observations are usually contaminated by noise. Before discussing how to deal with the data corrupted by noise, in this subsection we perform a brief perturbation analysis for problem (5). The analysis will provide us with some basic guidelines to handle the corrupted data.

Suppose A and X are perturbed by ΔA and ΔX , respectively. Let \hat{Z}^* be the minimizer to

$$\begin{aligned} \min_Z \quad & \|Z\|_*, \\ \text{s.t.} \quad & X + \Delta X = (A + \Delta A)Z. \end{aligned}$$

Then we want to analyze the influences of the perturbations ΔX and ΔA . Since $\text{rank}(\hat{Z}^*) = \text{rank}(X + \Delta X)$ (see Corollary 3.1), $\text{rank}(\hat{Z}^*)$ is invariant to ΔA , provided that ΔA is not very large such that $A + \Delta A$ is still able to span the data space. So the minimizer Z^* should not be very sensitive to ΔA . Whereas since $\text{rank}(X + \Delta X)$ will increase dramatically along with the increase of the perturbation level, the minimizer should be quite sensitive to ΔX . To verify, we present an example as the following.

Example 3.1: We construct a 100×200 dictionary matrix A that contains the basis of 10 independent subspaces each of which is of rank 10. So $\text{rank}(A) = 100$, i.e., A is of full row rank⁷. We construct a 100×200 data matrix X by sampling 200 data vectors from two out of those 10 subspaces such that $\text{rank}(X) = 20$. Some entries in X or A are randomly chosen to perturb by adding Gaussian noise with zero mean and variance 0.1. To measure the influences of the perturbations, we define *sensitivity* as:

$$\text{sensitivity} = \frac{\|\hat{Z}^* - Z^*\|}{\|Z^*\|}.$$

The results in Fig.4 show that the minimizer to problem (5) is much less sensitive to ΔA than ΔX . These results are consistent with our analysis above.

⁷It is worth noting that we actually need not assume that A is of full low rank, because Corollary 3.1 has shown that $\text{rank}(\hat{Z}^*) = \text{rank}(X + \Delta X)$ for any dictionary (provided that $X + \Delta X = (A + \Delta A)Z$ has feasible solutions). In this example, we create a full low rank dictionary just because it is relatively easy to make $X + \Delta X = (A + \Delta A)Z$ be feasible by using such a dictionary.

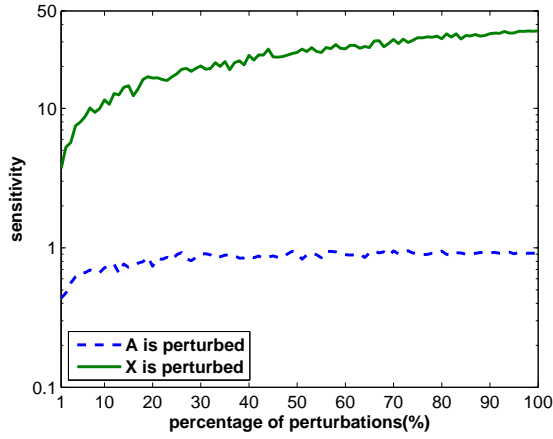


Fig. 4

SHOWING THE SENSITIVITY TO PERTURBATIONS. WE KEEP DATA X (OR DICTIONARY A) CLEAN AND COMPUTE THE *sensitivity* AT VARIOUS PERTURBATION LEVELS IN A (OR X), RESPECTIVELY.

C. Recovering Low-Rank Matrices by Convex Optimization

Theorem 3.1 suggests that it is appropriate to use the nuclear norm as a surrogate to replace the rank function in problem (3). Also, the analysis in Section III-B.3 shows that it is not difficult to obtain an “acceptable” dictionary A in advance. So we could obtain a low-rank recovery to X^0 by solving the following convex optimization problem:

$$\begin{aligned} \min_{Z, E} \quad & \|Z\|_* + \lambda \|E\|_{2,1}, \\ \text{s.t.} \quad & X = AZ + E. \end{aligned} \quad (12)$$

Here we adopt the ℓ_2/ℓ_1 -norm (1) to characterize the noise, as it fits well our assumptions⁸. After obtaining the minimizer (Z^*, E^*) , we could use AZ^* (or $X - E^*$) to obtain a low-rank recovery to the original data X^0 .

The problem (12) is convex and can be optimized by various methods. We first convert it to the following equivalent problem:

$$\begin{aligned} \min_{Z, E, J} \quad & \|J\|_* + \lambda \|E\|_{2,1}, \\ \text{s.t.} \quad & X = AZ + E, \\ & Z = J. \end{aligned}$$

This problem can be solved by the Augmented Lagrange Multiplier (ALM) method, which minimizes the following augmented Lagrange function:

$$\begin{aligned} & \|J\|_* + \lambda \|E\|_{2,1} + \text{tr}(Y_1^T(X - AZ - E)) \\ & + \text{tr}(Y_2^T(Z - J)) + \frac{\mu}{2}(\|X - AZ - E\|_F^2 + \|Z - J\|_F^2). \end{aligned}$$

The above problem is unconstrained. So it can be minimized with respect to J , Z and E , respectively, by fixing the other variables, and then updating the Lagrange multipliers Y_1 and Y_2 , where $\mu > 0$ is a penalty parameter. The inexact ALM method, also called the alternating direction method, is outlined in Algorithm 1. Its convergence properties could

⁸The ℓ_1 -norm can also be used. The performance is similar to that using ℓ_2/ℓ_1 -norm in our experiments on real data.

Algorithm 1 Solving Problem (12) by Inexact ALM

Input: data matrix X , parameter λ .

Initialize: $Z = J = 0, E = 0, Y_1 = 0, Y_2 = 0, \mu = 10^{-6}, \max_u = 10^6, \rho = 1.1$, and $\varepsilon = 10^{-8}$.

while not converged **do**

1. fix the others and update J by

$$J = \arg \min \frac{1}{\mu} \|J\|_* + \frac{1}{2} \|J - (Z + Y_2/\mu)\|_F^2.$$

2. fix the others and update Z by

$$Z = (\mathbf{I} + A^T A)^{-1} (A^T (X - E) + J + (A^T Y_1 - Y_2)/\mu).$$

3. fix the others and update E by

$$E = \arg \min \frac{\lambda}{\mu} \|E\|_{2,1} + \frac{1}{2} \|E - (X - AZ + Y_1/\mu)\|_F^2.$$

4. update the multipliers

$$Y_1 = Y_1 + \mu(X - AZ - E),$$

$$Y_2 = Y_2 + \mu(Z - J).$$

5. update the parameter μ by $\mu = \min(\rho\mu, \max_u)$.

6. check the convergence conditions:

$$\|X - AZ - E\|_\infty < \varepsilon \text{ and } \|Z - J\|_\infty < \varepsilon.$$

end while

be proved similarly as those in [35]. Notice that although Step 1 and Step 3 of the algorithm are convex problems, they both have closed-form solutions. Step 1 is solved via the Singular Value Thresholding (SVT) operator [36], while Step 3 is solved via the following lemma:

Lemma 3.5 ([37], Lemma 3.3): Let $Q = [q_1, q_2, \dots, q_i, \dots]$ be a given matrix. If the optimal solution to

$$\min_W \lambda \|W\|_{2,1} + \frac{1}{2} \|W - Q\|_F^2$$

is W^* , then the i -th column of W^* is

$$[W^*]_{:,i} = \begin{cases} \frac{\|q_i\|_2 - \lambda}{\|q_i\|_2} q_i, & \text{if } \lambda < \|q_i\|_2, \\ 0, & \text{otherwise.} \end{cases}$$

The major computation of Algorithm 1 is Step 1, which requires computing the SVD of an $m \times n$ matrix (assuming A and X are $d \times m$ and $d \times n$, respectively). So the complexity of the algorithm is $O(n^3)$. Nevertheless, it is possible to use partial SVD to reduce the complexity to $O(n^2)$ because it is unnecessary to compute the singular values/vectors that will be shrunk to zeros. Step 2 can also be made efficient by using the preconditioned conjugate gradient method [38]. We leave these as future work.

D. Discussions

Algorithm 2 Solving Problem (13) by Inexact ALM

Input: data matrix X , parameter λ .

Initialize: $Z = J = 0$, $E = 0$, $Y_1 = 0$, $Y_2 = 0$, $Y_3 = 0$, $\mu = 10^{-6}$, $max_u = 10^6$, $\rho = 1.1$, $\varepsilon = 10^{-8}$.

while not converged **do**

1. fix the others and update J by

$$J = \arg \min \frac{1}{\mu} \|J\|_* + \frac{1}{2} \|J - (Z + Y_2/\mu)\|_F^2.$$

2. fix the others and update Z by

$$\begin{aligned} Z &= (\mathbf{I} + A^T A + 1_m 1_m^T)^{-1} (1_m 1_n^T + A^T (X - E) + J \\ &+ (A^T Y_1 - Y_2 - 1_m Y_3)/\mu). \end{aligned}$$

3. fix the others and update E by

$$E = \arg \min \frac{\lambda}{\mu} \|E\|_{2,1} + \frac{1}{2} \|E - (X - AZ + Y_1/\mu)\|_F^2.$$

4. update the multipliers

$$\begin{aligned} Y_1 &= Y_1 + \mu(X - AZ - E), \\ Y_2 &= Y_2 + \mu(Z - J), \\ Y_3 &= Y_3 + \mu(1_m^T Z - 1_n^T). \end{aligned}$$

5. update the parameter μ by $\mu = \min(\rho\mu, max_u)$.

6. check the convergence conditions:

$$\|X - AZ - E\|_\infty < \varepsilon, \|Z - J\|_\infty < \varepsilon \text{ and } \|1_m^T Z - 1_n^T\|_\infty < \varepsilon$$

end while

1) *On Handling Affine Subspaces:* Sometimes the data may come from multiple affine rather than linear subspaces. In this case, as suggested by [19], we may tackle this issue by enforcing each column of Z sum to one:

$$\begin{aligned} \min_Z \quad & \|Z\|_*, \\ \text{s.t.} \quad & X = AZ, \\ & 1_m^T Z = 1_n^T, \end{aligned}$$

where 1_m and 1_n are vectors of all ones. For corrupted data, we just need to slightly modify the formulation (12) to

$$\begin{aligned} \min_{Z,E} \quad & \|Z\|_* + \lambda \|E\|_{2,1}, \\ \text{s.t.} \quad & X = AZ + E, \\ & 1_m^T Z = 1_n^T. \end{aligned} \quad (13)$$

This problem can be solved similarly as (12). For the completeness of presentation, we also outline the solution method in Algorithm 2.

As the affine spaces may not have a common point, the block-diagonal property (Theorem 3.2) is no longer valid⁹. Nevertheless, the problem (13) is convex and could be solved efficiently.

⁹Please note that the Theorem 2 in [19] is incorrect, because the homogeneous coordinate system has no definition for the zero point.

2) *On Characterizing the Noise:* Since the ℓ_2/ℓ_1 -norm (1) encourages the columns of E to be zero, the underlying assumption in (12) is that the noise is ‘‘sample-specific’’, i.e., some data vectors are corrupted and the others are clean. For a certain noise vector e (a column of E), its properties are characterized by the ℓ_2 -norm, which implicitly assumes that e may have a dense support. When it is known a priori that the noise vectors always have sparse supports, it is more suitable to adopt the ℓ_1 -norm regularization:

$$\begin{aligned} \min_{Z,E} \quad & \|Z\|_* + \lambda \|E\|_1, \\ \text{s.t.} \quad & X = AZ + E. \end{aligned} \quad (14)$$

The above problem can be solved analogously to problem (12), just replacing Step 3 of Algorithm 1 by

$$E = \arg \min \frac{\lambda}{\mu} \|E\|_1 + \frac{1}{2} \|E - (X - AZ + Y_1/\mu)\|_F^2,$$

which can be fulfilled by the shrinkage operator [35].

3) *Connection to Factorization Methods:* Factorization based methods build an affinity matrix by factorizing the data matrix and then applying spectral clustering to the affinity matrix for segmentation. This affinity matrix, which is called the Shape Interaction Matrix (SIM) [18] in computer vision, is defined as $\text{SIM}(X) = V_X V_X^T$ with $X = U_X \Sigma_X V_X^T$ being the skinny SVD of the data matrix X . Corollary 3.3 has clearly revealed the relationship between SIM and LRR. In summary, our LRR method generalizes the approach of SIM in two aspects: First, Theorem 3.1 suggests a way to define an affinity matrix between two different matrices; second, the formulations in (12), (13) and (14) provide methods to recover the affinity matrix from corrupted data.

IV. SUBSPACE RECOVERY BY LRR

In this section, we utilize LRR to address Problem 2.1, which is to recover a low-rank data matrix and a block-diagonal affinity matrix from a set of corrupted observation vectors. Let (Z^*, X^*) be a recovery produced by an algorithm, then we define *precision*, *recall* and *recovery error* to evaluate the quality of recovery:

$$\begin{aligned} \text{precision} &= \frac{\|G^0 \circ Z^*\|_0}{\|Z^*\|_0}, \\ \text{recall} &= \frac{\|G^0 \circ Z^*\|_0}{\|G^0\|_0}, \\ \text{recover error} &= \|X^0 - X^*\|_1, \end{aligned}$$

where \circ is the Hadamard product and G^0 is a mask matrix that indicates the true subspace membership:

$$[G^0]_{ij} = \begin{cases} 1, & \text{if } [X^0]_{:,i} \text{ and } [X^0]_{:,j} \text{ belong to} \\ & \text{the same subspace,} \\ 0, & \text{otherwise.} \end{cases}$$

Here we use G^0 as a surrogate of Z^0 , since it is impractical to know the exact definition of Z^0 . A recovery Z^* has high precision and recall means that it achieves large between-class margin (discrimination) and high within-class homogeneity, respectively. In order to achieve accurate segmentation, both precision and recall should be taken into account.

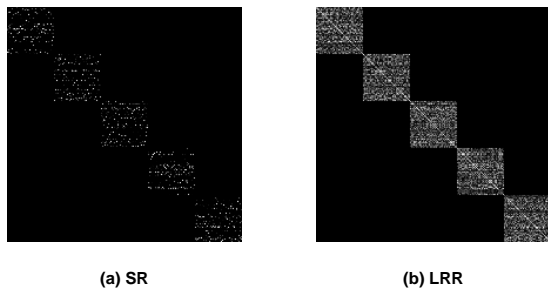


Fig. 5

COMPARING THE AFFINITY MATRICES PRODUCED BY SR AND LRR.

(A) THE AFFINITY MATRIX PRODUCED BY SR: $recall = 13\%$ AND $precision = 100\%$. (B) THE AFFINITY MATRIX PRODUCED BY LRR: $recall = 98\%$ AND $precision = 100\%$.

A. Choosing the Dictionary (Assumption 1)

By choosing the data matrix itself as the dictionary (i.e., $A = X$) in problem (5), Corollary 3.2 and Corollary 3.4 show that the minimizer Z^* naturally forms an affinity matrix that reveal the true data segmentation. Although these conclusions are obtained under the ideal assumption that the data is noiseless, they indicate that it may be a good choice to set $A = X$ ¹⁰. For more details about the affinity matrix identified by Z^* , we refer to the following example.

Example 4.1: We construct 5 independent subspaces $\{\mathcal{S}_i\}_{i=1}^5$ whose basis $\{U_i\}_{i=1}^5$ are computed by $U_{i+1} = TU_i$, $1 \leq i \leq 4$, where T is a random rotation and U_1 is a random column orthogonal matrix of dimension 100×4 . So each subspace has a rank of 4 and the data has an ambient dimension of 100. We construct a 100×200 data matrix $X = [X_1, \dots, X_5]$ by sampling 40 data vectors from each subspace by $X_i = U_i C_i$, $1 \leq i \leq 5$ with C_i being a 4×40 i.i.d. $\mathcal{N}(0, 1)$ matrix. Then we obtain a 200×200 affinity matrix by (7). For comparison, we also implement SR that computes an affinity matrix by minimizing

$$\begin{aligned} \text{(SR:)} \quad & \min_Z \quad \|Z\|_1, \\ & \text{s.t.} \quad X = XZ, \\ & \quad [Z]_{ii} = 0. \end{aligned}$$

Here, SR needs to enforce $[Z]_{ii} = 0$ to avoid the trivial solution $Z = \mathbf{I}$.

Fig.5 compares the affinity matrices produced by SR and LRR. It can be seen that LRR has the nature of both high within-class homogeneity (recall) and large between-class margin (precision). Whereas SR only achieves high between-class margin. Although there is no difference in their segmentation performance in this example (because the data is noiseless), as we will see, LRR can distinctly outperform SR while the data is grossly corrupted.

¹⁰Please note that it is not a unique choice to use $A = X$. We will discuss the other choices in our experiments.

B. Robustness to Sample-Specific Noise (Assumption 2)

In real applications, our observations are often noisy, or even grossly corrupted, and some observations may be missing. For small noise, a reasonable strategy is simply to relax the equality constraint in (5), similar to [39]. If we imagine instead that a fraction of the data vectors are grossly corrupted, the objective function in (12) might be more appropriate. By choosing $A = X$, we have the following optimization problem:

$$\begin{aligned} \min_{Z, E} \quad & \|Z\|_* + \lambda \|E\|_{2,1}, \\ \text{s.t.} \quad & X = XZ + E. \end{aligned} \quad (15)$$

After obtaining an optimal solution (Z^*, E^*) , we could recover the original data by using $X - E^*$ (or XZ^*) and obtain the segmentation results by using Z^* . To show how the noise is corrected, we refer to an example as follows.

Example 4.2: We construct two 1D subspaces \mathcal{S}_1 and \mathcal{S}_2 embedded in R^3 , and sample 40 data vectors from each subspace. About 32% of all those 80 data vectors are corrupted by large Gaussian noise with zero mean and a standard deviation of 0.4. For comparison, we implement the methods of RPCA and SR as follows:

$$\begin{aligned} \text{(RPCA:)} \quad & \min_{D, E} \quad \|D\|_* + \lambda \|E\|_1, \\ & \text{s.t.} \quad X = D + E, \end{aligned} \quad (16)$$

where the recovery is given by D^* (or $X - E^*$), in which (D^*, E^*) is the minimizer, and

$$\begin{aligned} \text{(SR:)} \quad & \min_{Z, E} \quad \|Z\|_1 + \lambda \|E\|_1, \\ & \text{s.t.} \quad X = XZ + E, \\ & \quad [Z]_{ii} = 0, \end{aligned} \quad (17)$$

where the recovery is given by $X - E^*$ (or XZ^*), with (Z^*, E^*) being the minimizer.

The results in Fig.6(d) and Fig.6(e) show that LRR¹¹ obtains a successful recovery of the subspace structures, including a good reconstruction of the original data (see Fig.6(d)) and an affinity matrix that is close to being block-diagonal (see Fig.6(e)). Since LRR is unlikely to cause “positive-false” to change the clean data, the possible noise could be corrected in such a way: Let’s rearrange the data vectors into $X = [X_l, X_c]$, where X_l is the clean data without noise and X_c is the corrupted data. In the case that the clean data X_l is still sufficient to represent the subspaces, and the noise is properly bounded, it will automatically correct the noise so as to obtain the lowest-rank representation. PRCA does not work well because it essentially ignores the difference between the data drawn from $\mathcal{S}_1 \oplus \mathcal{S}_2$ and the data drawn respectively from \mathcal{S}_1 and \mathcal{S}_2 .

C. Robustness to Full Noise (Assumption 3)

The real data always contains noise. Due to the varieties of the environment for acquiring data, the noise levels are also diverse among different observations. For example, the face

¹¹Since the noise has sparse supports, in this example LRR adopts ℓ_1 -regularization to characterize the noise.

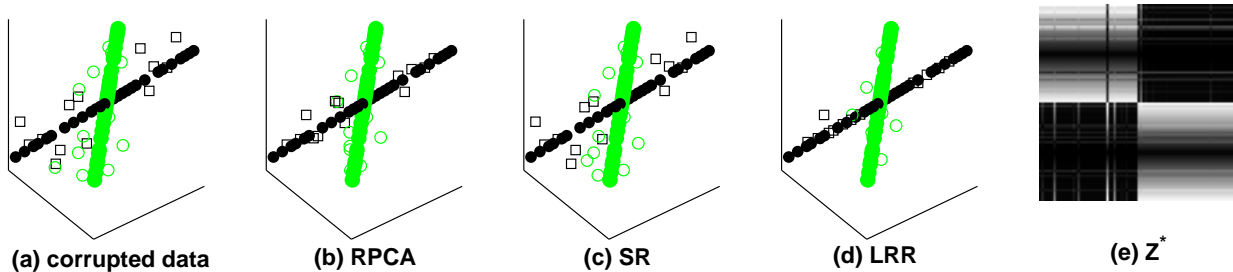


Fig. 6

COMPARING THE RECONSTRUCTION PERFORMANCE OF RPCA, SR AND LRR. (A) THE DATA; A PART OF WHICH IS CORRUPTED. (B) THE CORRECTED DATA PRODUCED BY RPCA ($\lambda = 0.21$, *recovery error*= 6.78). (C) THE CORRECTED DATA PRODUCED BY SR ($\lambda = 1.5$, *recovery error*= 8.50). (D) THE CORRECTED DATA PRODUCED BY LRR ($\lambda = 0.07$, *recovery error*= 5.46). (E) THE AFFINITY MATRIX PRODUCED BY LRR. FOR EACH METHOD, THE PARAMETER λ IS TUNED TO BE THE BEST WITH RESPECT TO THE RECOVERY ERROR.

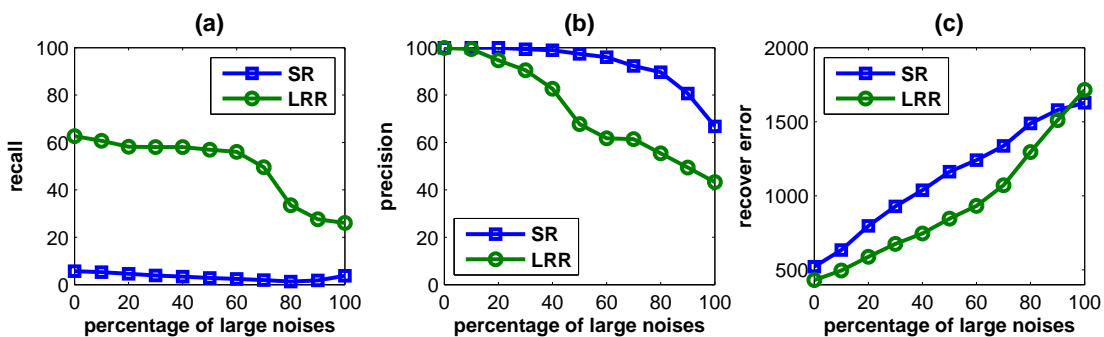


Fig. 7

COMPARING THE RECOVERY PERFORMANCE OF SR AND LRR. (A) RECALL VS. PERCENTAGE OF LARGE NOISE. (B) PRECISION VS. PERCENTAGE OF LARGE NOISE.. (C) RECOVERY ERROR VS. THE PERCENTAGE OF LARGE NOISE. THE PARAMETER λ IS TUNED TO OBTAIN THE BEST RECONSTRUCTION PERFORMANCE AT 30% PERCENT LARGE NOISE: $\lambda = 1.2$ FOR SR AND $\lambda = 0.9$ FOR LRR.

images taken under normal conditions are only contaminated by small noise, while the images pictured under extreme lighting conditions are grossly corrupted. So a suitable noisy model is that a fraction of data vectors are grossly corrupted and the others are contaminated by small noise, as suggested by our Assumption 3. In this case, since the dictionary A itself can defend some noise (as shown in Section III-B.3), we directly utilize the formulation (15) to deal with the data matrix of full noise. To investigate its performance, we show an example as in the following.

Example 4.3: We sample 200 data vectors from 5 independent subspaces constructed in the same way as in Example 4.1. Some data vectors are randomly chosen to be corrupted by using large Gaussian noise, and the rest are corrupted by using relatively small noise: If a data vector x is chosen to be corrupted by large noise, its observed vector is generated by adding Gaussian noise with zero mean and standard deviation $0.2\|x\|_2$; otherwise, its observed vector is generated by adding small Gaussian noise with standard deviation $0.01\|x\|_2$ ($\|x\|_2$ mostly ranges from 0.1 to 1.7 in this experiment).

Fig. 7 shows the evaluation results in terms of recall, precision and recovery error. Although SR always obtains high precision scores, its recall is much lower (below 6%). Since

Algorithm 3 Subspace Segmentation by LRR

Input: data matrix X , number of subspaces k .

1. obtain the minimizer Z^* to problem (15) by Algorithm 1.
 2. construct an undirected graph by using $|Z^*| + |(Z^*)^T|$ as the affinity matrix of the graph.
 3. use Normalized Cut to segment the vertices of the graph into k clusters.
-

both recall and precision are important for accurate segmentation, SR may not produce accurate segmentation results, as we will see in the next section. Moreover, LRR also outperforms SR for recovering the original data.

D. The Subspace Segmentation Algorithm

The results in Fig. 7 also illustrate that our current method may not obtain a strictly block-diagonal affinity matrix. It is even asymmetric. So we need a postprocessing step to obtain the final segmentation. After solving problem (15), as in [19], [20], we utilize the affinity matrix (denoted by Z^*) to define edge weights of an undirected graph. The data vectors correspond to the vertices and the edge weight between x_i

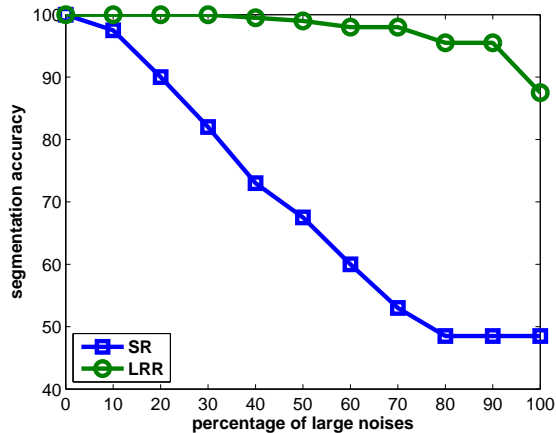


Fig. 8

COMPARING THE SEGMENTATION PERFORMANCE OF SR AND LRR.

WE PLOT THE SEGMENTATION ACCURACY ACROSS THE ENTIRE RANGE OF LARGE NOISE FOR THE TWO METHODS. LRR CLEARLY OUTPERFORMS SR, PERFORMING NEARLY PERFECTLY UP TO 70 PERCENT LARGE NOISE.

THE PARAMETERS ARE THE SAME AS THOSE IN FIG. 7.

and x_j is defined as $|[Z^*]_{ij}| + |[Z^*]_{ji}|$. We could then use the spectral clustering algorithms such as Normalized Cuts (NCut) [28] to produce the final segmentation results. Algorithm 3 summarizes the whole segmentation algorithm of LRR. To see the segmentation performance, we refer to the following example.

Example 4.4: We construct 200 corrupted data vectors in the same way as Example 4.3. At each level of large noise, we use Algorithm 3 to segment the data into 5 clusters and record the *segmentation accuracy*¹². For comparison, we also include the results of SR, which computes the affinity matrix by solving problem (17).

Fig. 8 shows that LRR performs nearly perfectly up to 70 percent large noise. These results do not conflict with those in Fig. 7, since the NCut method could also help defend some noise. As SR always results in a very low recall (see Fig. 7(a)), its segmentation performance is rather disappointing in this example. These experimental results also verify that the real mechanism of SR is not to model the generic subspace structures (one may refer to Fig. 2).

V. EXPERIMENTS

In this section, we test LRR on real segmentation tasks. Some previous state-of-the-art methods are also included.

A. Results on Hopkins155

We evaluate LRR on the Hopkins155 motion database [40]. The database consists of 156 sequences each of which has

¹²As clustering methods cannot provide the class label for each cluster, we use a postprocess step to assign each cluster a label: Given ground truth classification results, the label of a cluster is the index of the ground truth class that contributes the maximum number of samples to the cluster. Then we can obtain the segmentation accuracy by computing the percentage of correctly classified data vectors.

TABLE I
SEGMENTATION ERRORS (%) ON HOPKINS155. THE PARAMETER OF LRR IS SET AS $\lambda = 2.4$. THE PARAMETERS OF ALL METHODS ARE TUNED TO BE THE BEST BY USING THE PCA DATA.

Raw Data						
	GPCA	LSA	RANSAC	SIM	SR	LRR
Mean	NA	8.99	8.22	5.25	3.89	3.16
Std.	NA	9.80	10.26	8.64	7.70	5.99
Max	NA	37.74	47.83	48.74	32.57	37.43
PCA 12D						
	GPCA	LSA	RANSAC	SIM	SR	LRR
Mean	30.51	8.77	7.81	5.08	3.66	3.13
Std.	11.79	9.80	9.72	8.57	7.21	5.96
Max	55.67	38.37	41.31	48.74	37.44	32.50
State-of-the-art: [3]						
Mean	3.37					

39~550 data vectors drawn from two or three motions (a motion corresponds to a subspace). Each sequence is a sole clustering (segmentation) task and so there are 156 clustering tasks in total. Since the outliers in the data have been manually removed, it could be regarded that this database only contains small noise.

1) *Main Results:* We test two settings on this database. The first one is based on using the raw data without any preprocessing. In the second setting, since the rank of data must be bounded above by 12 [19], we use a preprocessing step to project the data to be 12D by PCA. In order to compare LRR with the state of the art, we also list the results of GPCA, Local Subspace Analysis (LSA) [2], RANSAC, SIM and SR. Table I shows that LRR significantly outperforms GPCA, LSA, RANSAC and SIM, and also outperforms SR. This confirms that the lowest-rank criterion is accurate for modeling the structures of subspaces. Moreover, the preprocessing step also slightly improves the performance of LRR. This is natural because the data should be relatively easier to handle if its noise level has been reduced successfully in advance.

Compared to the state-of-the-art algorithms for motion segmentation, the performance of LRR is also quite competitive. For example, by choosing an appropriate projection dimension and an appropriate distortion parameter, the motion segmentation method proposed in [3] can achieve a segmentation error of 3.37% (see Table 2 of [3]). This benchmark has been outperformed by our LRR, which can achieve 3.16% without any preprocessing and 3.13% with an extra dimension reduction step.

2) *Performance of Various Configurations:* The formulation (15) is not a unique choice to compute the affinity matrix. There are several optional configurations of LRR, e.g., we could enforce each column of Z to sum to one for better handling affine subspaces, and adopt the ℓ_1 -norm rather than the ℓ_2/ℓ_1 -norm to characterize a different type of noise. In this subsection, we will test the performance of these different configurations and investigate the influences of the parameter λ .

The parameter $\lambda > 0$ is used to balance the effects of the two parts in problem (12) (and problems (13), (14) and (15)). In general, the choice of this parameter depends on the prior

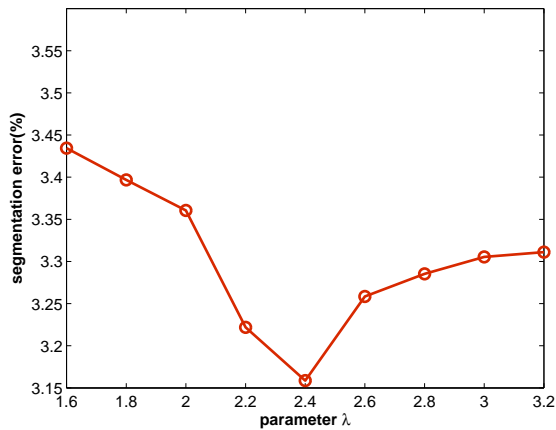


Fig. 9

THE INFLUENCES OF THE PARAMETER λ . WE PLOT THE SEGMENTATION ERROR (%) OF LRR AS A FUNCTION OF THE PARAMETER λ . THESE EXPERIMENTS ARE PERFORMED BY USING THE RAW DATA WITHOUT ANY PREPROCESSING.

knowledge on the noise level of data. When the noise is slight, we should use relatively large λ ; when the noise is heavy, we should set λ to be relatively small. Nevertheless, LRR could work well under a wide range of parameter settings, as shown in Fig.9. While λ ranges from 1.6 to 3.2, the segmentation error varies slightly from 3.15% to 3.45%.

Actually, the data of a motion should lie on a 3D affine subspace. However, the formulation (12) actually treats the motion as a 4D linear subspace. So we had better use formulation (13), where the dictionary A is chosen as the data matrix X itself. This formulation works slightly better than (15). For example, when using the PCA data and choosing $\lambda = 2.4$, we obtain a segmentation error of 3.12%, which is slightly better than the 3.13% produced by using (15).

As mentioned in Section III-D.2, the ℓ_1 -norm could also be used to characterize the noise E^0 . So we also consider formulation (14) with $A = X$. When using the raw data and setting $\lambda = 2.2$, the above formulation produces a segmentation error of 3.27%, which is close to the 3.16% produced by (15).

3) *Influences of Choosing the Dictionary:* It is not a unique choice to use the data matrix X itself as the dictionary. In general, LRR could perform better if we can obtain a relatively “cleaner” dictionary A . Here, we consider and compare the following three mechanisms.

Mechanism 1. Using the data matrix X itself as the dictionary, i.e., $A = X$.

Mechanism 2. Using the processed data by PCA, i.e., $A = UU^T X$, where U is formed by the first 12 principal components of X .

Mechanism 3. Using the processed data by RPCA, i.e., $A = D^*$, where D^* is the minimizer (with regard to the variable D) of problem (16). The parameter of RPCA is set to be $\lambda = 0.3$ in our experiments.

Table II shows the segmentation performance of using the above three mechanisms to define the dictionary A . It can

TABLE II
SEGMENTATION ERRORS (%) UNDER VARIOUS CHOICES OF THE DICTIONARY. THESE EXPERIMENTS ARE DONE BY USING THE RAW DATA WITHOUT ANY PREPROCESSING. THE PARAMETER OF LRR IS $\lambda = 2.4$.

	Mechanism 1	Mechanism 2	Mechanism 3
Segmentation Error	3.158	3.152	3.140

TABLE III
SEGMENTATION ACCURACIES (%) ON EXTENDED YALE DATABASE B. WE HAVE TUNED THE PARAMETERS OF ALL METHODS TO THE BEST.

Raw Data ($\lambda = 0.16$ for LRR)						
	GPCA	LSA	RANSAC	SIM	SR	LRR
Accuracy	NA	31.72	NA	15.94	37.66	62.53
PCA 200D (no normalization, $\lambda = 0.16$ for LRR)						
	GPCA	LSA	RANSAC	SIM	SR	LRR
Accuracy	NA	38.44	32.19	51.25	40.16	67.50
PCA 200D (normalized, $\lambda = 1.6$ for LRR)						
	GPCA	LSA	RANSAC	SIM	SR	LRR
Accuracy	NA	32.81	25.32	49.53	62.03	61.41

be seen that RPCA works slightly better than the other two mechanisms. This is because RPCA is usually better than PCA as a tool for removing noise in data. Nevertheless, it has no significant advantage to use RPCA to construct the dictionary, since the solution is not very sensitive to the noise in the dictionary, as shown in Section III-B.3.

B. Results on Extended Yale Database B

We test LRR’s ability to cope with large noise in data, using a part of Extended Yale Database B [41], which consists of 640 frontal face images of 10 classes (there are 38 classes in the whole database and we use the first 10 classes for experiments). Each class contains about 64 images. We resize the images into 42×48 and use the raw pixel values to form data vectors of dimension 2016. As shown in Fig.10, more than half of the data vectors have been corrupted by “shadows” and noise. So the noise level in this database is quite high.

The first sub-table of Table III shows the results obtained by using the raw data without any preprocessing. It can be seen that LRR distinctly outperforms the baselines. The advantages of LRR mainly comes from its ability of automatically correcting the noise in data, as shown in Fig.11. Here the principle is to recover the original data with the assistant of a dictionary A that also contains noise ($A = X$ in this example).



Fig. 10

EXAMPLES OF THE IMAGES OF A CLASS IN EXTENDED YALE DATABASE B.

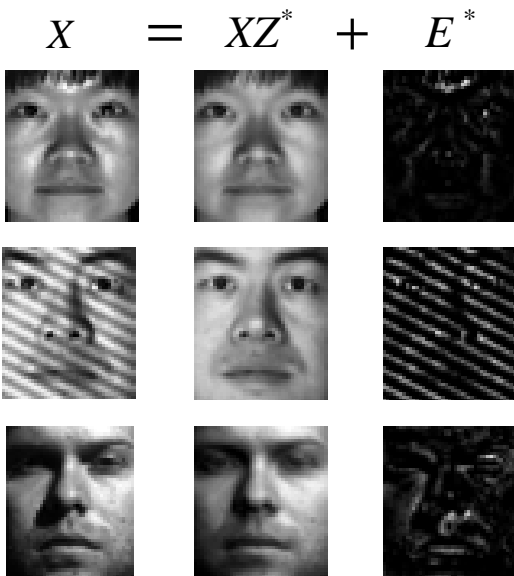


Fig. 11

SOME EXAMPLES OF USING LRR TO CORRECT THE CORRUPTIONS IN FACES. LEFT: THE ORIGINAL DATA (X); MIDDLE: THE CORRECTED DATA (XZ^*); RIGHT: THE ERROR (E^*).

The second sub-table of Table III shows the performance of various methods by using the 200D data produced by PCA. Again, LRR distinctly outperforms the baselines. To better fit the assumptions of SR, we try to normalize the data vectors to have unit lengths, that is, to transform the subspaces into “bouquet-like” structures (Fig.2). The third sub-table of Table III shows that SR achieves the best performance in this case. This phenomena verifies that the real mechanism of SR is a bouquet model as shown in Fig.2. Moreover, the segmentation performance of LRR (and all the other methods except SR) is reduced by the normalization operator. This is natural, because it can damage the linear structures to normalize the data vectors to a unit ball. It is also worth noting that it is the small variance of face images (see the first row of Fig.10) that enables the success of normalization. For the data that has standard subspace structures (e.g., Fig.1, Fig.6 and Example 4.3), the normalization operator may fail.

VI. CONCLUSION

In this paper we propose low-rank representation (LRR) to identify the subspace structures from corrupted data. Namely, our goal is to segment the samples into their respective subspaces and correct the possible noise simultaneously. LRR is a generalization of the recently established PRCA method, extending the recovery of corrupted data from single subspace to multiple subspaces. Also, LRR generalizes the approach of SIM, giving a way to define an affinity matrix between two different matrices, and providing a mechanism to recover an affinity matrix from corrupted data. Compared to the previous methods that solely target data segmentation, LRR integrates data segmentation and noise correction into a unified framework so as to achieve a more accurate segmentation. Both

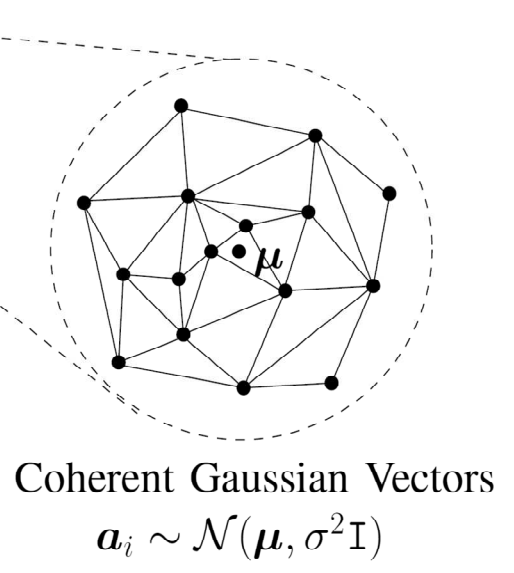
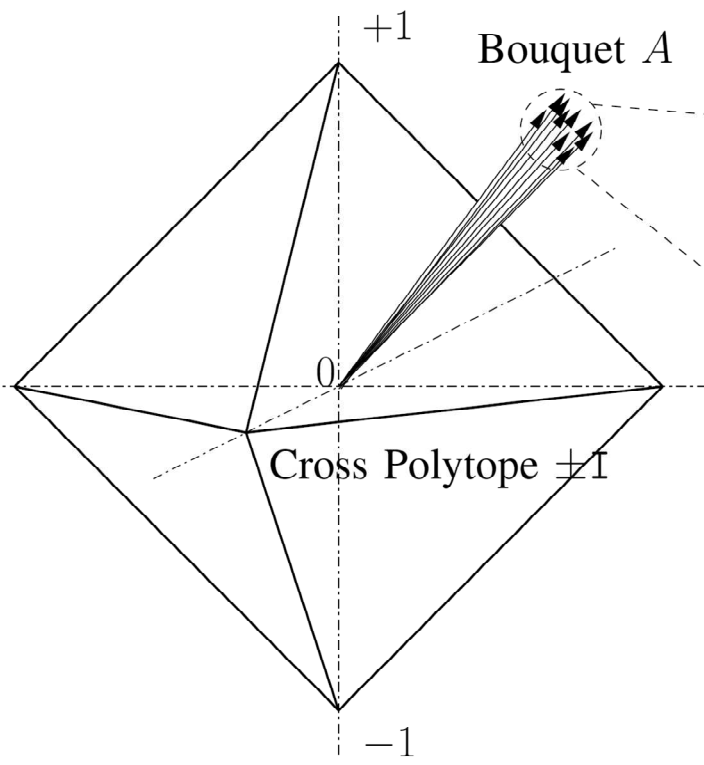
theoretical and experimental results show the effectiveness of LRR. However, there remain several problems for future work:

- It will be better to learn a compact dictionary for LRR, which is to recover the structure that generates the data. The analysis in Section III-B.3 does not deny the importance of learning the dictionary, but instead shows that the selection of dictionary is a bottleneck to further improve the performance.
- LRR also gives a way to recover the corrupted data drawn from multiple subspaces. The theoretical conditions for the success of the recovery should be established.
- The subspace segmentation should not be the only application of LRR. By choosing appropriate dictionaries, the method of LRR could fit various applications well.
- Our current method is still unable to recover a strictly block-diagonal affinity matrix from corrupted data. Some additional constraints may be applied to problem (12), e.g., the semi-definite constraint suggested by [33].
- Our current optimization algorithm is not very efficient for large scale databases. More scalable algorithms should be developed.

REFERENCES

- [1] C. W. Gear, “Multibody grouping from motion images,” *International Journal on Computer Vision*, vol. 29, no. 2, pp. 133–150, 1998.
- [2] J. Yan and M. Pollefeys, “A general framework for motion segmentation: Independent, articulated, rigid, non-rigid, degenerate and non-degenerate,” in *European Conference on Computer Vision*, vol. 4, 2006, pp. 94–106.
- [3] S. Rao, R. Tron, R. Vidal, and Y. Ma, “Motion segmentation in the presence of outlying, incomplete, or corrupted trajectories,” *IEEE Transactions on Pattern Analysis and Machine Intelligence*, vol. 32, no. 10, pp. 1832–1845, 2010.
- [4] J. Wright, A. Y. Yang, A. Ganesh, S. S. Sastry, and Y. Ma, “Robust face recognition via sparse representation,” *IEEE Transactions on Pattern Analysis and Machine Intelligence*, vol. 31, pp. 210–227, 2008.
- [5] Y. Ma, H. Derksen, W. Hong, and J. Wright, “Segmentation of multivariate mixed data via lossy data coding and compression,” *IEEE Transactions on Pattern Analysis and Machine Intelligence*, vol. 29, no. 9, pp. 1546–1562, 2007.
- [6] J. Mercer, “Functions of positive and negative type, and their connection with the theory of integral equations,” *Philosophical Transactions of the Royal Society*, vol. 209, pp. 415–446, 1909.
- [7] E. J. Candès and B. Recht, “Exact matrix completion via convex optimization,” *Foundations of Computational Mathematics*, vol. 9, no. 6, pp. 717–772, 2009.
- [8] R. Keshavan, A. Montanari, and S. Oh, “Matrix completion from noisy entries,” in *Advances in Neural Information Processing Systems*, 2009, pp. 952–960.
- [9] J. Wright, A. Ganesh, S. Rao, Y. Peng, and Y. Ma, “Robust principal component analysis: Exact recovery of corrupted low-rank matrices via convex optimization,” in *Advances in Neural Information Processing Systems*, 2009, pp. 2080–2088.
- [10] R. H. Keshavan, A. Montanari, and S. Oh, “Matrix completion from noisy entries,” *Journal of Machine Learning Research*, vol. 11, pp. 2057–2078, 2010.
- [11] J. Ho, M.-H. Yang, J. Lim, K.-C. Lee, and D. J. Kriegman, “Clustering appearances of objects under varying illumination conditions,” in *IEEE Conference on Computer Vision and Pattern Recognition*, vol. 1, 2003, pp. 11–18.
- [12] G. Liu, Z. Lin, X. Tang, and Y. Yu, “Unsupervised object segmentation with a hybrid graph model (HGM),” *IEEE Transactions on Pattern Analysis and Machine Intelligence*, vol. 32, no. 5, pp. 910–924, 2010.
- [13] M. A. Fischler and R. C. Bolles, “Random sample consensus: a paradigm for model fitting with applications to image analysis and automated cartography,” *Commun. ACM*, vol. 24, no. 6, pp. 381–395, 1981.
- [14] J. Wright and Y. Ma, “Dense error correction via l1-minimization,” *IEEE Transactions on Information Theory*, vol. 56, no. 7, pp. 3540–3560, 2010.

- [15] L. Lu and R. Vidal, "Combined central and subspace clustering for computer vision applications," in *International conference on Machine learning*, 2006, pp. 593–600.
- [16] K. Huang and S. Aviyente, "Sparse representation for signal classification," in *Advances in Neural Information Processing Systems*, 2006, pp. 609–616.
- [17] C. Zhang and R. R. Bitmead, "Subspace system identification for training-based mimo channel estimation," *Automatica*, vol. 41, no. 9, pp. 1623–1632, 2005.
- [18] a. P. Costeira, Jo and T. Kanade, "A multibody factorization method for independently moving objects," *International Journal on Computer Vision*, vol. 29, no. 3, pp. 159–179, 1998.
- [19] E. Elhamifar and R. Vidal, "Sparse subspace clustering," in *IEEE Conference on Computer Vision and Pattern Recognition*, vol. 2, 2009, pp. 2790–2797.
- [20] G. Liu, Z. Lin, and Y. Yu, "Robust subsapce segmentation by low-rank represnetation," in *International Conference on Machine Learning*, 2010, pp. 663–670.
- [21] E. J. Candès, X. Li, Y. Ma, and J. Wright, "Robust principal component analysis?" *Submitted to Journal of the ACM*, 2009.
- [22] A. Gruber and Y. Weiss, "Multibody factorization with uncertainty and missing data using the EM algorithm," in *IEEE Conference on Computer Vision and Pattern Recognition*, vol. 1, 2004, pp. 707–714.
- [23] T. Zhang, A. Szlám, and G. Lerman, "Median k-flats for hybrid linear modeling with many outliers," in *IEEE International Workshop on Subspace Methods*, 2009.
- [24] A. Yang, S. Rao, and Y. Ma, "Robust statistical estimation and segmentation of multiple subspaces," in *Workshop of IEEE Conference on Computer Vision and Pattern Recognition*, 2006.
- [25] J. Wright, Y. Tao, Z. Lin, Y. Ma, and H.-Y. Shum, "Classification via minimum incremental coding length (MICL)," in *Advances in Neural Information Processing Systems*, 2008.
- [26] Y. Ma, A. Yang, H. Derksen, and R. Fossum, "Estimation of subspace arrangements with applications in modeling and segmenting mixed data," *SIAM Review*, vol. 50, no. 3, pp. 413–458, 2008.
- [27] S. Rao, A. Yang, S. Sastry, and Y. Ma, "Robust algebraic segmentation of mixed rigid-body and planar motions in two views," *International Journal on Computer Vision*, vol. 88, no. 3, pp. 425–446, 2010.
- [28] J. Shi and J. Malik, "Normalized cuts and image segmentation," *IEEE Transactions on Pattern Analysis and Machine Intelligence*, pp. 888–905, 2000.
- [29] Y. C. Eldar and M. Mishali, "Robust recovery of signals from a structured union of subspaces," *IEEE Transactions on Information Theory*, vol. 55, no. 11, pp. 5302–5316, 2009.
- [30] M. Fazel, "Matrix rank minimization with applications," *PhD thesis*, 2002.
- [31] Z. Zhang, X. Liang, A. Ganesh, and Y. Ma, "TILT: Transform invariant low-rank textures," in *Assian Conference on Computer Vision*, 2010.
- [32] S. Wei and Z. Lin, "Analysis and improvement of low rank representation for subspace segmentation," *submitted to IEEE Transactions on Signal Processing*, 2010.
- [33] J. Sun, Y. Ni, X. Yuan, S. Yan, and L.-F. Cheong, "Robust low-rank subspace segmentation with semidefinite guarantees," in *ICDM Workshop on Optimization Based Methods for Emerging Data Mining Problems*, 2010.
- [34] B. Recht, W. Xu, and B. Hassibi, "Necessary and sufficient conditions for success of the nuclear norm heuristic for rank minimization," CalTech Technical Report (<http://www.ist.caltech.edu/~brecht/papers/08.RecXuHas.TR.pdf>), Tech. Rep.
- [35] Z. Lin, M. Chen, L. Wu, and Y. Ma, "The augmented Lagrange multiplier method for exact recovery of corrupted low-rank matrices," UIUC Technical Report UILU-ENG-09-2215, Tech. Rep., 2009.
- [36] J.-F. Cai, E. J. Candès, and Z. Shen, "A singular value thresholding algorithm for matrix completion," *SIAM Journal on Optimization*, vol. 20, no. 4, pp. 1956–1982, 2010.
- [37] J. Yang, W. Yin, Y. Zhang, and Y. Wang, "A fast algorithm for edge-preserving variational multichannel image restoration," *SIAM Journal on Imaging Sciences*, vol. 2, no. 2, pp. 569–592, 2009.
- [38] G. H. Golub and C. F. Van Loan, *Matrix computations (3rd ed.)*. Baltimore, MD, USA: Johns Hopkins University Press, 1996.
- [39] E. J. Candès and Y. Plan, "Matrix completion with noise," in *IEEE Proceeding*, vol. 98, 2010, pp. 925–936.
- [40] R. Tron and R. Vidal, "A benchmark for the comparison of 3-d motion segmentation algorithms," in *IEEE Conference on Computer Vision and Pattern Recognition*, 2007, pp. 1–8.
- [41] K. Lee, J. Ho, and D. Kriegman, "Acquiring linear subspaces for face recognition under variable lighting," *IEEE Transactions on Pattern Analysis and Machine Intelligence*, vol. 27, no. 5, pp. 684–698, 2005.



Coherent Gaussian Vectors
 $\mathbf{a}_i \sim \mathcal{N}(\boldsymbol{\mu}, \sigma^2 \mathbf{I})$